Pictorial Essay

http://dx.doi.org/10.3348/kjr.2012.13.3.332
pISSN 1229-6929 · eISSN 2005-8330
Korean J Radiol 2012;13(3):332-341

Korean Journal of Radiology
KJR

Practical Application of Iterative Decomposition of Water and Fat with Echo Asymmetry and Least-Squares Estimation (IDEAL) Imaging in Minimizing Metallic Artifacts

Jang Gyu Cha, MD, Hyun Sook Hong, MD, Jai Soung Park, MD, Sang Hyun Paik, MD, Hae Kyung Lee, MD

All authors: Department of Radiology, Soonchunhyang University Bucheon Hospital, Bucheon 420-767, Korea

Iterative decomposition of water and fat with echo asymmetry and the least-squares estimation (IDEAL) is a recently developed method for robust separation of fat and water with very high signal-to-noise-ratio (SNR) efficiency. In contrast to conventional fat-saturation methods, IDEAL is insensitive to magnetic field (B0 and B1) inhomogeneity. The aim of this study was to illustrate the practical application of the IDEAL technique in reducing metallic artifacts in postoperative patients with metallic hardware. The IDEAL technique can help musculoskeletal radiologists make an accurate diagnosis particularly in musculoskeletal imaging by reducing metallic artifacts, enabling the use of contrast enhancement, improving SNR performance, and providing various modes of MR images with one scan parameter.

Index terms: *MR; Musculoskeletal; MR artifact; Postoperative imaging*

INTRODUCTION

Magnetic resonance (MR) imaging is widely used for the assessment of postoperative complications. However, in daily practice, radiologists frequently encounter metallic-hardware-related problems including susceptibility artifacts and incomplete fat saturation in the evaluation of postoperative patients with metallic hardware (1-3). Furthermore, with the increasing use of high-field-strength MR imaging in clinical practice, this problem has become more challenging to radiologists (3). The Iterative decomposition of water and fat with echo asymmetry and the least-squares estimation (IDEAL) technique offers robust fat saturation. Recently, this technique has been presented as an alternative solution for metal-related artifacts (4, 5). In this article, we introduce the various practical applications of the IDEAL technique in reducing metallic artifacts in postoperative patients with metallic hardware.

Received July 28, 2011; accepted after revision October 6, 2011.
Corresponding author: Jang Gyu Cha, MD, Department of Radiology, Soonchunhyang University Bucheon Hospital, 170 Jomaru-ro, Wonmi-gu, Bucheon 420-767, Korea.
• Tel: (8232) 621-5851 • Fax: (8232) 621-5874
• E-mail: mj4907@schmc.ac.kr

How are Metallic Artifacts Presented in the MR Image?

Metal-related artifacts created by metallic hardware are evident in four different forms (Fig. 1) (1, 4). First, the spins may be mapped to an erroneous location within the image, resulting in the distortion of the shape of the metallic object along the axes of frequency encoding and section selection (1). Second, a complete signal loss may be observed around the metallic object, as the local magnetic field is so strong that the spins are almost immediately dephased (6). Third, a rim of high signal intensity may be present around the metallic devices as a result of the mismapping of a disproportionate number of spins to that location. The resultant misregistration effect mainly occurs in the direction of frequency encoding (1). Finally, depending on the composition and size of the metallic

Korean Journal of Radiology
KJR

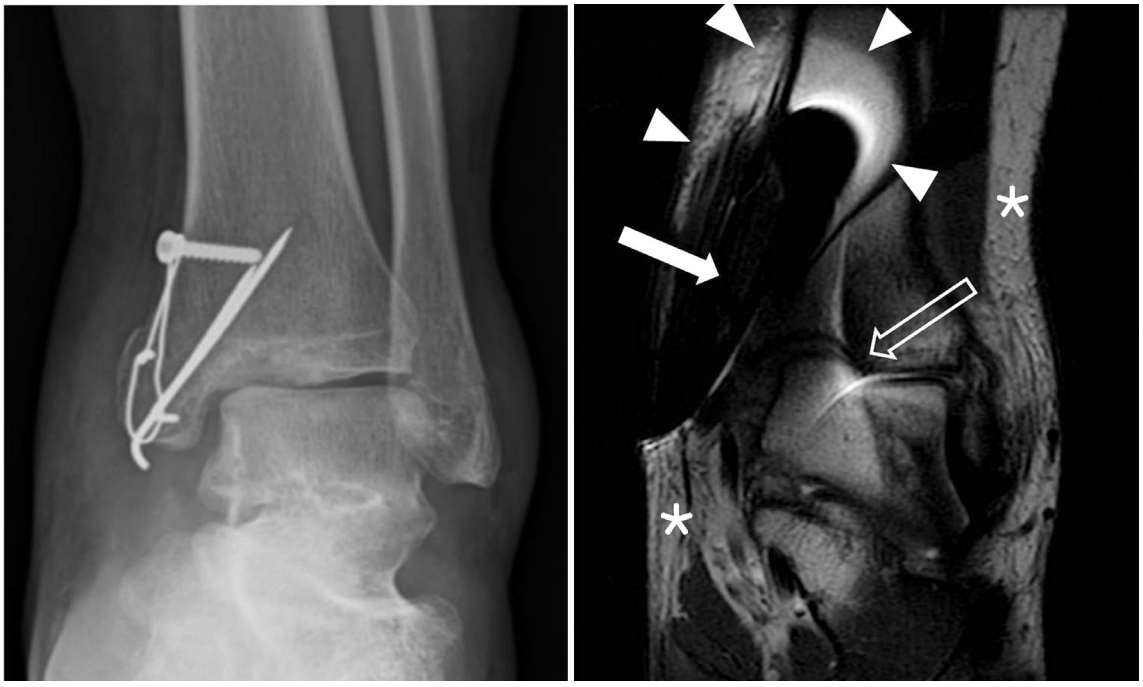

A B

Fig. 1. Forms of metallic artifacts caused by metallic hardware in left ankle joint (3.0 T, TR/TE = 4633/75, field of view [FOV] = 14 cm, slice = 3 mm, echo train length [ETL] = 11, echo spacing = 14.1, bandwidth [BW] = 41,67 kHz, matrix = 384 x 256, acquisition time = 2 min 52 sec).
A. Ankle anterior-posterior view reveals tension-band wire fixation device inserted in medial melleolus of distal tibia. **B.** Frequency-selected fat saturated (FSFS) T2-weighted image shows area of complete signal void (solid arrow), geographic distortion of tibiotalar joint (open arrow), peripheral high-signal lesions around metallic implant (arrowheads), and incomplete fat saturation (asterisks).

device, incomplete fat saturation resulting from the local magnetic field may affect an area surrounding the metallic hardware larger than that affected by another type of artifact, resulting in widespread suboptimal fat saturation throughout the multiple sequential images (1, 4).

Practical Remedies for Metallic Artifacts

Many practical remedies have been suggested to alleviate metallic artifacts. The susceptibility artifacts from metallic devices can be readily reduced by adjusting the sequence parameters by using a small field of view, a high-resolution matrix, thin sections, increased readout bandwidth, and a higher echo-train length (1, 7, 8). Additionally, swapping the phase and frequency encoding may be helpful, particularly when specific anatomic areas are obscured by the metal artifact (8).

STIR Imaging

Short-inversion-time inversion-recovery (STIR) imaging has been proposed as a solution to susceptibility artifacts as it is relatively independent of the homogeneity of the main magnetic field (1, 2). However, STIR imaging is not suited for contrast-enhanced imaging because short T1 tissues with a T1 similar to that of fat are likely to be suppressed. Furthermore, the overall potency of STIR imaging is limited due to its dependence on the inversion pulse and relatively long TI (180-220 ms). STIR also generates partial saturation of the target tissue signal, which significantly reduces the signal-to-noise-ratio (SNR) performance (4, 5, 9).

What is IDEAL Imaging?

The IDEAL technique using a three-point water-fat separation method was designed to provide uniform fat saturation while maintaining a high SNR (5, 10, 11). Although several fat saturation techniques using three-point approaches with symmetric echoes were already introduced to reduce the time between refocusing pulses of the FSE train, these techniques can suffer when a voxel includes water and fat in an almost similar proportion (11). However, this problem was solved with the advent of IDEAL imaging, which is a three-point method using asymmetric echoes and least-squares fitting (11).

For robust fat saturation, this technique employs an

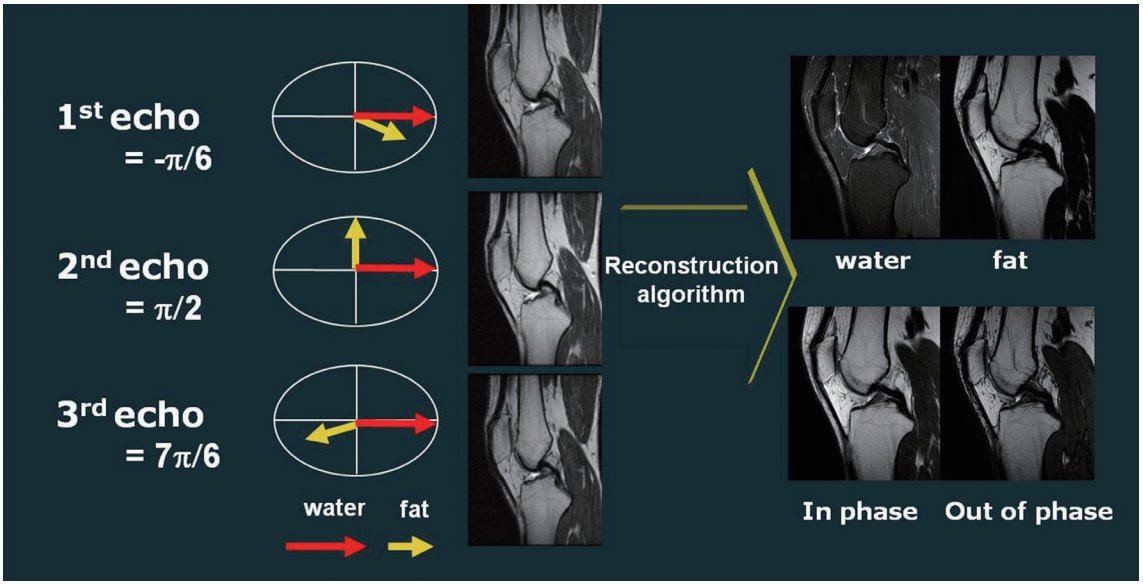

Fig. 2. Schematic showing process of obtaining three images in asymmetric manner at phase between water and fat in quadrature (i.e., perpendicular). 120° phase before and after quadrature images, serve to produce water-only, fat-only, in-phase, and out-of-phase images using recombination algorithm.

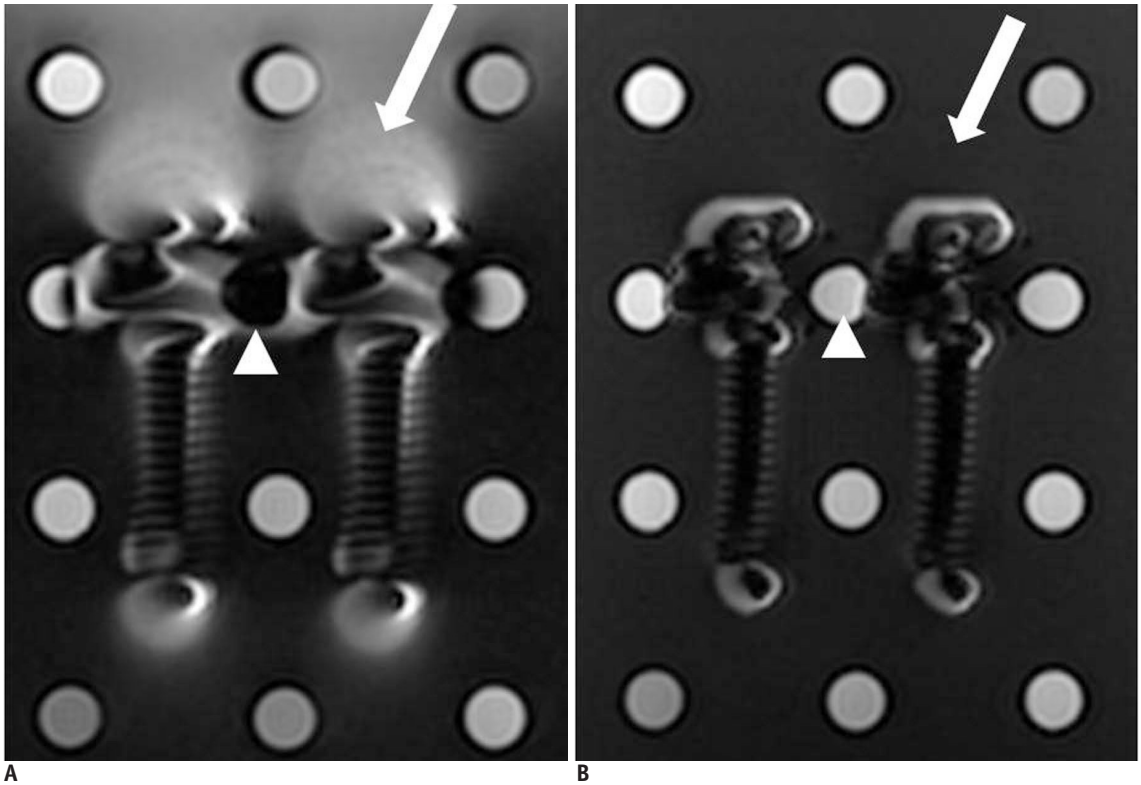

Fig. 3. MR images of spinal pedicle screws placed between test tubes filled with diluted gadolinium contrast material in phantom filled with oil.
A. Fat-saturated T1-weighted (1.5 T, TR/TE = 500/15, FOV = 24 cm, slice = 2 mm, ETL = 7, echo spacing = 11.5, BW = 31.25 kHz , matrix = 256 x 256, acquisition time = 1 min 07 sec) and **(B)** IDEAL T1-weighted images (1.5 T, TR/TE = 500/15, FOV = 24 cm, slice = 2 mm, ETL = 8, echo spacing = 13.3, BW = 31.25 kHz , matrix = 256 x 256, acquisition time = 3 min 37 sec) show area of peripheral high-signal-intensity lesions around pedicle screws (arrow), with marked decreased in IDEAL T1-weighted images compared with fat-saturated T1-weighted images. IDEAL T1-weighted images show that signal intensity of contrast material in test tube between pedicle screws (arrowhead) is maintained against metallic artifacts, whereas fat-saturated T1-weighted images reveal complete loss of signal intensity in test tube (arrowhead).

Korean Journal of Radiology
KJR

iterative approach to estimate the field map and remove its effects from the water-fat decomposition as well as a region-growing algorithm to prevent fat-water ambiguities that can lead to fat-water "swapping" (5, 12).

Additionally, the IDEAL technique also allows for the optimization of echo shifts to obtain an image with the phase between the water and fat in quadrature and an image with a phase 120° before and 120° after the quadrature image (13) (Fig. 2).

These features enable the IDEAL technique to be resistant to magnetic field (B0 and B1) inhomogeneity, especially when encountering metallic hardwares in postoperative imaging.

Clinical Utility

Decrease in Metallic Artifacts

In previous studies, IDEAL imaging has proven highly effective in the reduction of metallic artifacts compared with the frequency-selective fat-saturation technique (FSFS) (4). The results of this study (4) reveal that the decrease in metallic artifacts was greatest for the peripheral

Fig. 4. 41-year-old man with posterior interpedicular screw fixation in L5.
Fat-saturated axial T2 **(A)** (1.5 T, TR/TE = 4000/102, field of view = 18 cm, slice = 4 mm, ETL = 11, echo spacing = 14.1, BW = 41.67 kHz , matrix = 320 x 224, acquisition time = 3 min 04 sec) and contrast-enhanced T1-weighted images **(C)** (1.5 T, TR/TE = 750/12, FOV = 18 cm, slice = 4 mm, ETL = 5, echo spacing = 9.5, BW = 41.67 kHz ,matrix = 320 x 224, acquisition time = 4 min 37 sec) show that dural sac (arrow) is not visualized due to metallic artifacts caused by pedicular screws, whereas the whole area of dural sac is fully depicted on IDEAL T2- **(B)** (1.5 T, TR/TE = 400/102, FOV = 18 cm, slice = 4 mm, ETL = 24, echo spacing = 11.9, BW = 41.67kHz, matrix = 320 x 224 , acquisition time = 7 min 12 sec) and contrast-enhanced T1-weighted images **(D)** (1.5 T, TR/TE = 750/12, FOV = 18 cm, slice = 4 mm, ETL = 16, echo spacing = 12.3, BW = 41.67 kHz, matrix = 320 x 224, acquisition time = 5 min 16 sec). Note that circumferential epidural enhancement along dural sac (arrowheads), which is not observed on fat saturated contrast-enhanced T1-weighted images, is clearly visualized on IDEAL T1-weighted images **(D)**.

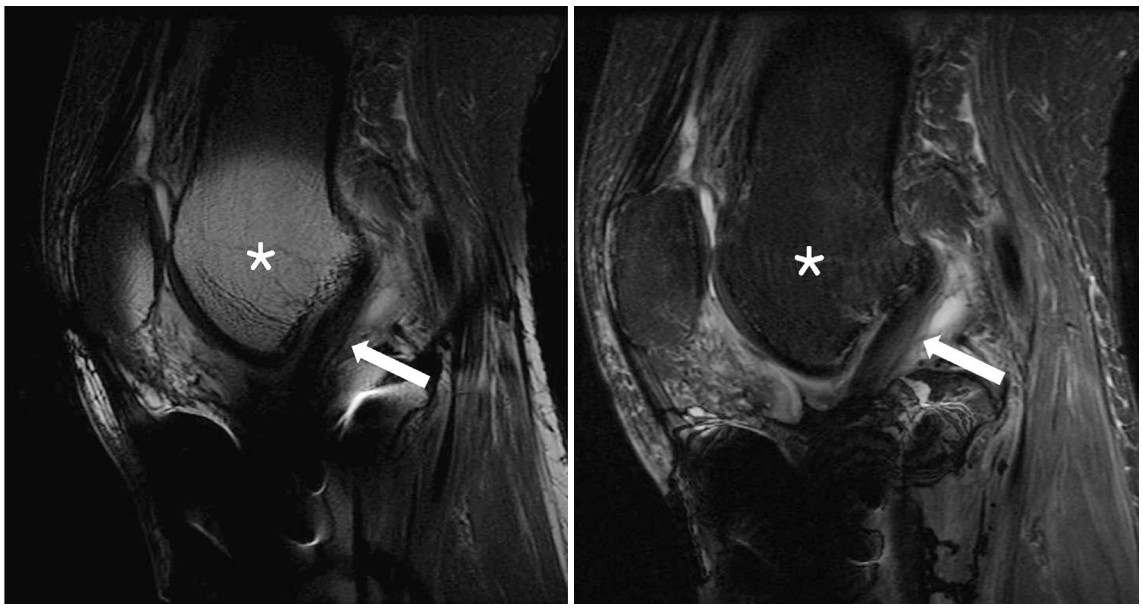

Fig. 5. 34-year-old man with cancellous screw fixation in right proximal tibia.
In fat-saturated T2-weighted images **(A)** (3.0 T, TR/TE = 4000/72, FOV = 16 cm, slice = 3.5 mm, ETL = 10, echo spacing = 14.1, BW = 41.67 kHz, matrix = 512 x 256, acquisition time = 2 min 46 sec), metallic artifact from metallic implant in proximal tibia is observed as high-signal-intensity lesion (asterisk) affecting distal femur and patella. Inferior portion of anterior cruciate ligament is obscured by signal-loss artifact from implant (arrow), and IDEAL T2-weighted images **(B)** (3.0 T, TR/TE = 4000/72, FOV = 16 cm, slice = 3.5 mm, ETL = 11, echo spacing = 12.2, BW = 41.67 kHz, matrix = 512 x 256, acquisition time = 5 min 36 sec) demonstrate homogeneous low signal intensity in bone marrow, providing clearer visualization of entire portion of anterior cruciate ligament (arrow).

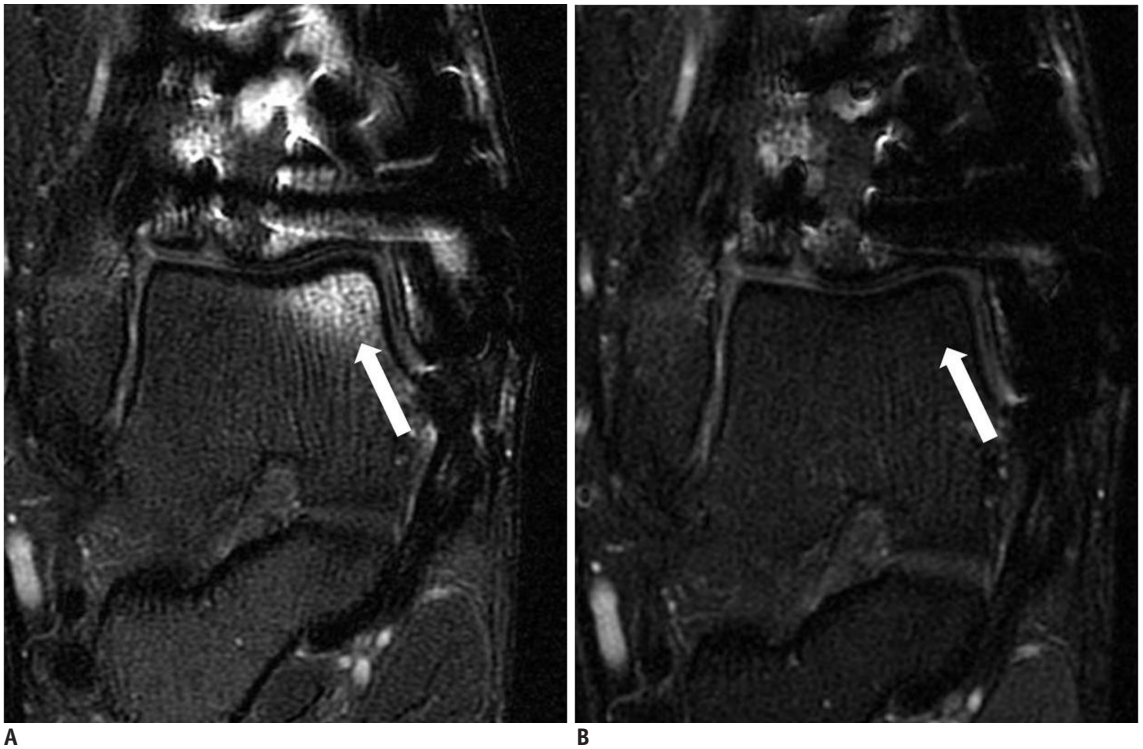

Fig. 6. 29-year-old man with open reduction internal fixation in right distal tibia.
Fat-saturated coronal T2-weighted images **(A)** (3.0 T, TR/TE = 4500/68, FOV = 14 cm, slice = 3 mm, ETL = 11, echo spacing = 13.2, BW = 41.67 kHz, matrix = 384 x 256, acquisition time = 2 min 58 sec) show high-signal-intensity lesion in subchondral area of medial talar dome (arrow), simulating osteochondral lesion, which is clearly removed on IDEAL T2-weighted images (arrow) **(B)** (3.0 T, TR/TE = 4500/68, FOV = 14 cm, slice = 3 mm, ETL = 11.6, echo spacing = 3,3, BW = 41.67 kHz, matrix = 384 x 256, acquisition time = 4 min 33 sec).

Korean Journal of Radiology
KJR

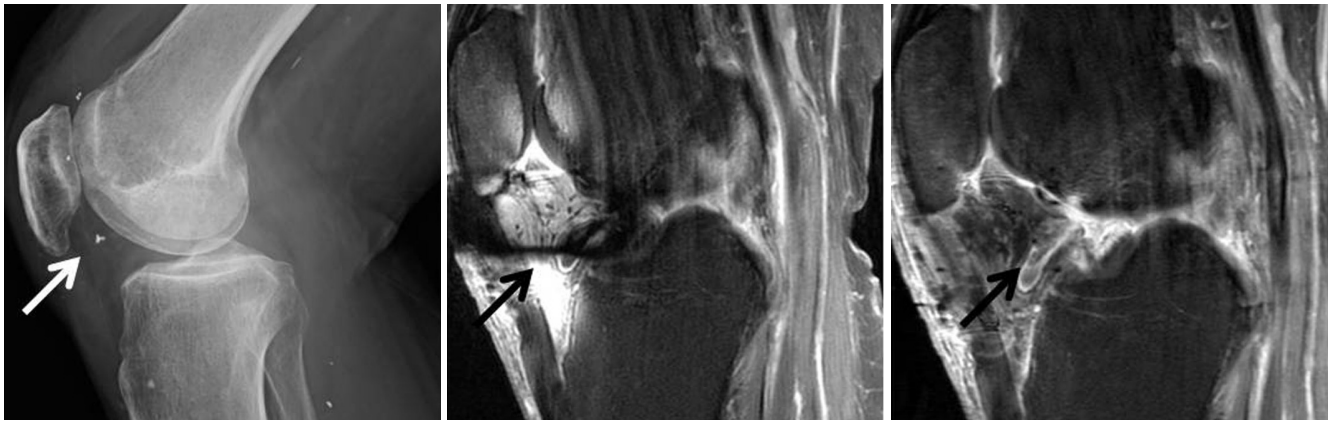

A B C

Fig. 7. 66-year-old man with metallic foreign body in his right knee joint.
Lateral radiography of right knee joint **(A)** shows tiny T-shaped fragment in patellofemoral joint. Significant metallic artifacts caused by metallic foreign body are shown in infrapatellar fat pad on contrast-enhanced sagittal T1-weighted images **(B)** (3.0 T, TR/TE = 800/12, FOV = 16 cm, slice = 3.5 mm, ETL = 4, echo spacing = 11.7, BW = 41.67 kHz, matrix = 384 x 256, acquisition time = 2 min 12 sec), whereas lower level of metallic artifact is observed in IDEAL contrast-enhanced T1 -weighted images **(C)** (3.0 T, TR/TE = 700/15, FOV = 16 cm, slice = 3.5 mm, ETL = 4, echo spacing = 10.6, BW = 31.25 kHz, matrix = 384 x 256, acquisition time = 4 min 33 sec).

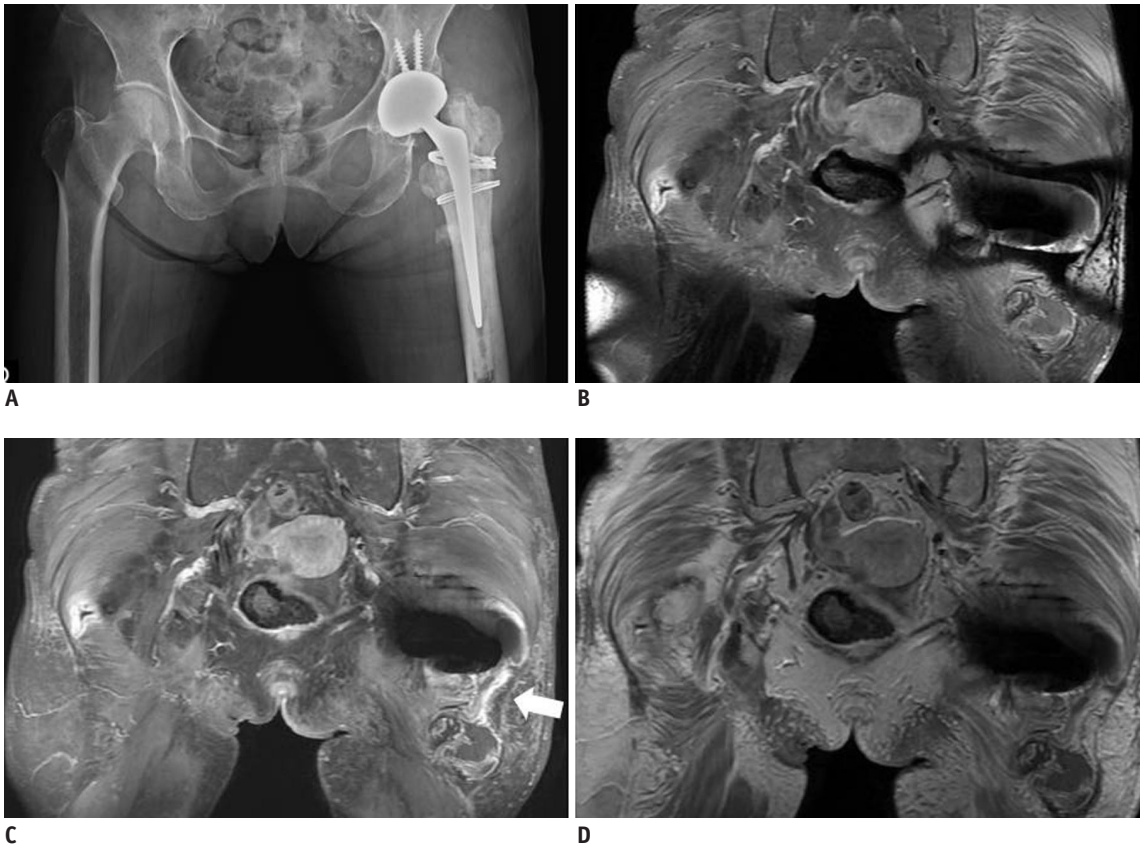

A B C D

Fig. 8. 79-year-old woman that underwent total hip arthroplasty in left hip joint.
Anteroposterior (AP) radiography of pelvis **(A)** shows total hip prosthesis in left hip joint. Coronal contrast-enhanced T1-weighted images **(B)** (3.0 T, TR/TE = 880/15, FOV = 40 cm, slice = 4 mm, ETL = 3, echo spacing = 14.1, BW = 41.67kHz , matrix = 416 x 224 , acquisition time = 4 min 21 sec) demonstrate significant susceptibility artifact around metallic implant and abscess, with marginal enhancement (arrow) located at inferior aspect of left hip joint. However, this image does not provide information about relationship between metallic implant and abscess. In contrast, IDEAL contrast-enhanced T1-weighted images (C) (3.0 T, TR/TE = 700/15, FOV = 40 cm, slice = 4 mm, ETL = 3, echo spacing = 12.9, BW = 41.67kHz, matrix = 416 x 224, acquisition time = 7 min 19 sec) and fat-water fusion images **(D)**, which are similar to non-saturated contrast-enhanced T1-weighted images, and reveal connection between total hip prosthesis and marginal enhanced abscess (arrowheads), with marked decreased metallic artifact.

rim of the high signal intensity surrounding the metallic devices (Fig. 3). Therefore, the use of IDEAL imaging allows superior visualization of the region of interest close to the metallic implants such as the dural sac in the spine (Fig. 4) or the intra-articular structures (Fig. 5) (4, 5, 10). IDEAL imaging can help eliminate potential false-positive high-signal-intensity lesions produced by the metallic hardware, which simulate bone marrow edema a soft tissue contusion, serving to avoid unnecessary studies or treatments (10) (Figs. 5, 6). Additionally, IDEAL imaging may facilitate the accurate assessment of the signal, such as the shape or size of the metallic materials, by minimizing artifacts (Fig. 7) as well as providing additional information regarding the relationship between the internal structures and the metallic materials.

Compatibility with the Use of Contrast Enhancement

In contrast to STIR imaging, the IDEAL technique

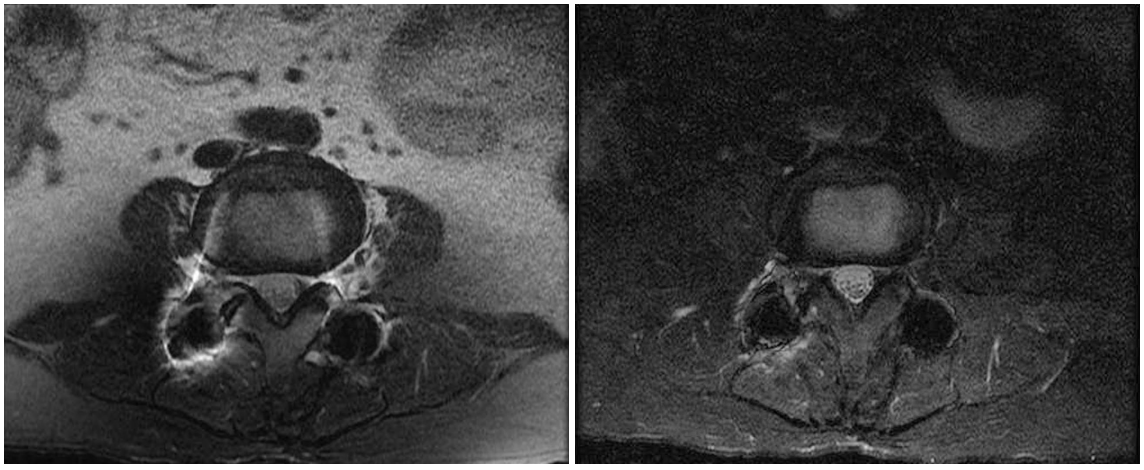

A B

Fig. 9. 64-year-old woman who underwent posterior fixation surgery at L3-L4 due to spinal stenosis.
Axial fat-saturated T2-weighted images **(A)** (1.5 T, TR/TE = 4000/102, field of view = 18 cm, slice = 4 mm, ETL = 11, echo spacing = 13.6, BW = 41.67 kHz , matrix = 320 x 224, acquisition time = 3 min 4 sec) show incomplete fat saturation caused by metallic interpedicular screws involving areas of subcutaneous and peritoneal fat. In contrast, axial IDEAL T2-weighted image (B) (1.5 T, TR/TE = 4000/102, field of view = 18 cm, slice = 4 mm, ETL = 24, echo spacing = 11.9, BW = 41.67 kHz, matrix = 320 x 224, acquisition time = 7 min 12 sec) shows homogeneous fat saturation within field of view.

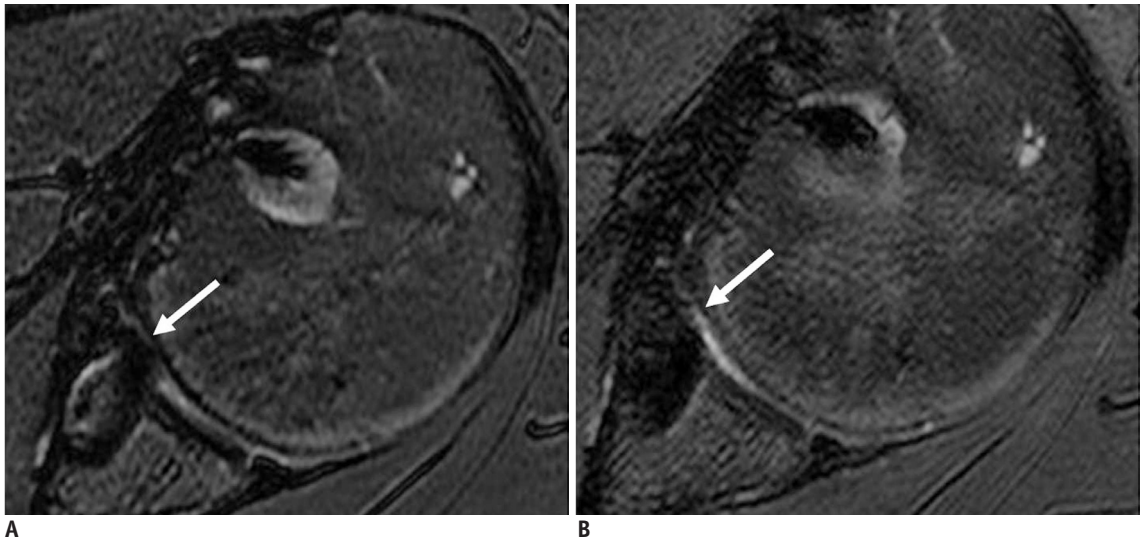

A B

Fig. 10. 56-year-old man performed with bankart repair 2 years previous.
Axial fat suppressed T2-weighted MR images **(A)** (3.0 T, TR/TE = 4000/68, FOV = 16 cm, slice = 2 mm, ETL = 8, echo spacing = 15.3, BW = 31.25 kHz, matrix = 320 x 224, acquisition time = 3 min 50 sec) shows that metallic artifact (arrows) from suture anchors in anteroinferior glenoid quadrant which hinders evaluation of glenohumeral joint. Axial IDEAL T2 -weighted MR images **(B)** (3.0 T, TR/TE = 4000/68, FOV = 16 cm, slice = 2 mm, ETL = 8, echo spacing = 13, BW = 31.25 kHz, matrix = 320 x 224, acquisition time = 6 min 11 s) depicts decreased artifact (arrow), rendering clear view of joint space.

Korean Journal of Radiology
KJR

has the strong advantage of offering contrast-enhanced imaging, which is essential for postoperative evaluation in patients suspected of having complications (4, 5) (Figs. 4, 8). Therefore, the IDEAL technique combined with contrast enhancement provides radiologists with a useful postoperative imaging option.

Uniform Fat Saturation

IDEAL imaging can provide consistent, robust fat saturation in musculoskeletal imaging, maintaining its own signal intensity of the tissue against the alteration of the magnetic field inhomogeneities from the metallic devices and also against the susceptibility differences created by

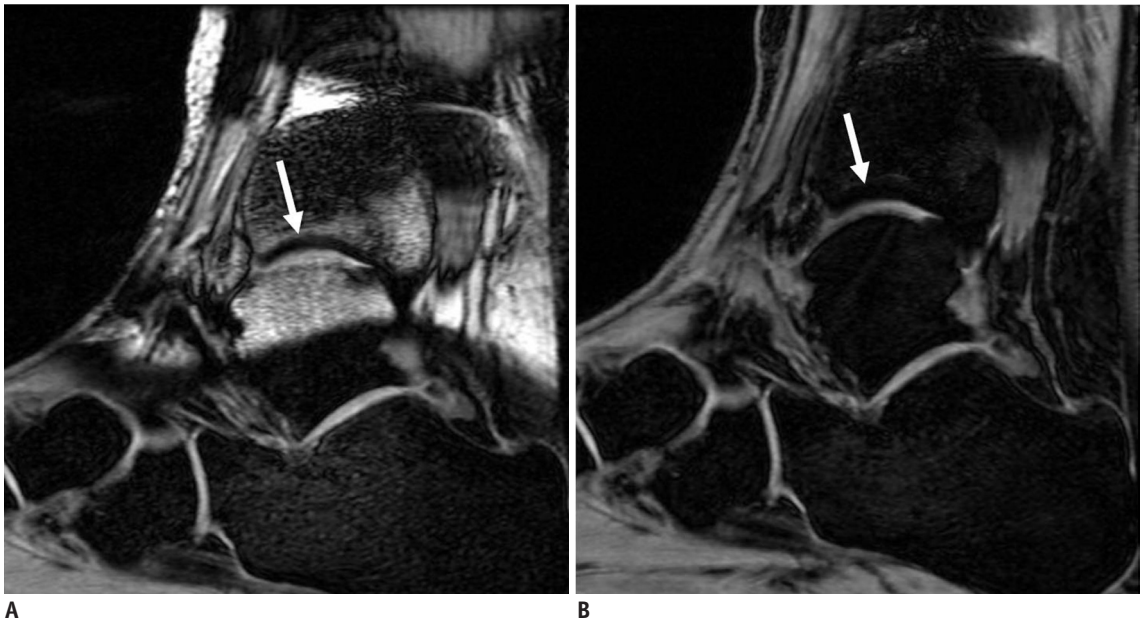

A B

Fig. 11. 43-year-old woman with open reduction internal fixation on both malleoli of left ankle joint.
Sagittal fat suppressed three-dimensional spoiled gradient echo (3D SPGR) MR images **(A)** (3.0 T, TR/TE = 17/4, FOV = 14 cm, flip angle = 25, slice = 2 mm, echo spacing = 4.3, BW = 15.63 kHz , matrix = 320 x 224 , acquisition time = 3 min 34 sec) shows that susceptibility artifact from metallic implants obscures tibiotalar joint (arrow). Sagittal IDEAL 3D SPGR MR images **(B)** (3.0 T, TR/TE = 14/4, FOV = 14 cm, flip angle = 25, slice = 2 mm, echo spacing = 4.6, BW = 15.63 kHz, matrix = 320 x 224, acquisition time = 8 min 26 sec) improves visualization of articular cartilage in tibiotalar joint (arrow).

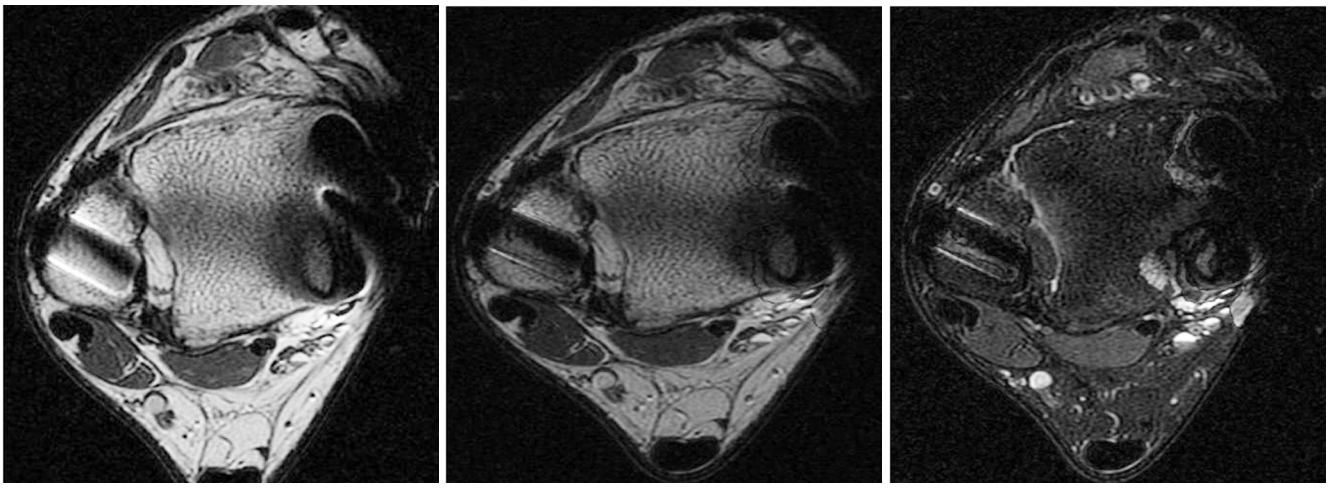

A B C

Fig. 12. 33-year-old man with tension-band fixation in medial malleolus and external fixation in lateral malleolus of left ankle.
Axial T2-weighted images obtained at level of tibiofibular ligament **(A)** (3.0 T, TR/TE = 4000/68, FOV = 14 cm, slice = 3 mm, ETL = 7, echo spacing = 13.2, BW = 41.67 kHz, matrix = 384 x 256, acquisition time = 3 min 36 sec) show susceptibility artifacts in both malleolar areas. Corresponding axial IDEAL T2-weighted recombined image **(B)** (3.0 T, TR/TE = 4000/68, FOV = 14 cm, slice = 3 mm, ETL = 7, echo spacing = 11.6, BW = 41.67 kHz , matrix = 384 x 256, acquisition time = 5 min 36 sec) shows image similar to T2-weighted image with decrease in metallic artifact. Note that water-only image **(C)** can be acquired without any additional scan time.

the sharp geometric variation of the extremities, including off-isocenter imaging and a large fields of view, which may facilitate an accurate interpretation of postoperative MR images (2, 4, 5) (Fig. 9).

Cartilage Imaging

Two-dimensional fast SE imaging (2D FSE) and three-dimensional spoiled gradient-echo (3D SPGR) imaging are the MR techniques most frequently applied in clinical practice for the assessment of cartilaginous lesions in the knee joints (14). However, when used in patients with orthopedic metallic devices in or around the joint spaces, the visualization of articular cartilage on MR imaging may be impeded by metallic artifacts. Furthermore, 3D SPGR can be more vulnerable to the susceptibility artifact than spin-echo images. IDEAL 2D FSE (Fig. 10) and IDEAL 3D SPGR (Fig. 11) are relatively insensitive to alterations in the magnetic field and display a high SNR efficiency, ultimately providing a superior image quality for articular cartilage, even in the challenging magnetic-field environment of joint imaging (14).

The Use of Additional Obtained Recombined Images

Besides water-only and fat-only images, recombined images including in-phase (water + fat) and out-of-phase (water - fat) images could be acquired following the correction for chemical shift artifacts in the readout direction (5, 10). This allows radiologists to exploit non-fat saturated images, which are primarily used for the evaluation of the anatomy without an additional MR scan in daily practice (15) (Figs. 8, 12).

Limitation of IDEAL Imaging

A shortcoming of IDEAL imaging is the need of longer scanning time than conventional FSE imaging does, because three acquisitions are indispensable for producing IDEAL images (11). Parallel imaging is considered as a possible remedy to reduce scanning time for IDEAL imaging without the loss of SNR, because the IDEAL technique has a very high SNR efficiency (11).

CONCLUSION

IDEAL is of great value as an MR imaging technique in postoperative patients with metallic hardware and can help musculoskeletal radiologists to make an accurate diagnosis by reducing metallic artifacts, which results in enabling the use of contrast enhancement, improving SNR performance, and providing various modes of MR images for each scan.

REFERENCES

1. Lee MJ, Kim S, Lee SA, Song HT, Huh YM, Kim DH, et al. Overcoming artifacts from metallic orthopedic implants at high-field-strength MR imaging and multi-detector CT. *Radiographics* 2007;27:791-803
2. Murakami M, Mori H, Kunimatsu A, Abe O, Chikuda H, Ono T, et al. Postsurgical spinal magnetic resonance imaging with iterative decomposition of water and fat with echo asymmetry and least-squares estimation. *J Comput Assist Tomogr* 2011;35:16-20
3. Harris CA, White LM. Metal artifact reduction in musculoskeletal magnetic resonance imaging. *Orthop Clin North Am* 2006;37:349-359, vi
4. Cha JG, Jin W, Lee MH, Kim DH, Park JS, Shin WH, et al. Reducing metallic artifacts in postoperative spinal imaging: usefulness of IDEAL contrast-enhanced T1- and T2-weighted MR imaging--phantom and clinical studies. *Radiology* 2011;259:885-893
5. Gerdes CM, Kijowski R, Reeder SB. IDEAL imaging of the musculoskeletal system: robust water fat separation for uniform fat suppression, marrow evaluation, and cartilage imaging. *AJR Am J Roentgenol* 2007;189:W284-W291
6. Zhuo J, Gullapalli RP. AAPM/RSNA physics tutorial for residents: MR artifacts, safety, and quality control. *Radiographics* 2006;26:275-297
7. Berquist TH. Imaging of the postoperative spine. *Radiol Clin North Am* 2006;44:407-418
8. Vandevenne JE, Vanhoenacker FM, Parizel PM, Butts Pauly K, Lang RK. Reduction of metal artefacts in musculoskeletal MR imaging. *JBR-BTR* 2007;90:345-349
9. Bydder GM, Steiner RE, Blumgart LH, Khenia S, Young IR. MR imaging of the liver using short TI inversion recovery sequences. *J Comput Assist Tomogr* 1985;9:1084-1089
10. Fuller S, Reeder S, Shimakawa A, Yu H, Johnson J, Beaulieu C, et al. Iterative decomposition of water and fat with echo asymmetry and least-squares estimation (IDEAL) fast spin-echo imaging of the ankle: initial clinical experience. *AJR Am J Roentgenol* 2006;187:1442-1447
11. Reeder SB, Pineda AR, Wen Z, Shimakawa A, Yu H, Brittain JH, et al. Iterative decomposition of water and fat with echo asymmetry and least-squares estimation (IDEAL): application with fast spin-echo imaging. *Magn Reson Med* 2005;54:636-644
12. Yu H, Reeder SB, Shimakawa A, Brittain JH, Pelc NJ. Field map estimation with a region growing scheme for iterative 3-point water-fat decomposition. *Magn Reson Med* 2005;54:1032-1039
13. Reeder SB, Wen Z, Yu H, Pineda AR, Gold GE, Markl M, et al. Multicoil Dixon chemical species separation with an iterative least-squares estimation method. *Magn Reson Med*

2004;51:35-45
14. Crema MD, Roemer FW, Marra MD, Burstein D, Gold GE, Eckstein F, et al. Articular cartilage in the knee: current MR imaging techniques and applications in clinical practice and research. *Radiographics* 2011;31:37-61
15. Leffler S, Disler DG. MR imaging of tendon, ligament, and osseous abnormalities of the ankle and hindfoot. *Radiol Clin North Am* 2002;40:1147-1170